

Coefficient of Thermal Expansion Characterization for Plain Polyethylene Pipe

Hanakumbo Mwanang'onze¹, Ian D. Moore², Mark Green³

Abstract

Situations arise in practice where axial forces induced by temperature changes can lead to failure of high-density polyethylene (HDPE) pipes. Temperature decreases can induce large axial tensions, and lead to fracture in the pipe barrel or at connections. Temperature increases can produce axial thrusts that induce buckling when there is insufficient lateral support along the pipe. The behavior of HDPE under thermal loading is therefore investigated for thick and thin-walled extruded pipe specimens. Experimental work has been performed to characterize the coefficients of thermal expansion in the longitudinal and circumferential directions. Testing was conducted to study the variability of the coefficients of thermal expansion over the temperature range -10°C to $+20^{\circ}\text{C}$. Further testing was conducted to investigate the dependence of thermal strain on thermal loading history. The data obtained from the experimental work have been used to implement thermal modeling capability in an existing linear viscoelastic (LVE) finite element model, to be reported on in a future paper.

Introduction

HDPE possesses many characteristics that make it attractive as a material from which to fabricate pipelines. Among these are resistance to chemical corrosion, toughness and ease of fabrication. However, because the use of HDPE in pipeline design has only come about relatively recently, there is a lack of understanding of several design issues. In some instances this has led to inadequate design and subsequent structural failure, while in other instances, to over-conservative and cost-inefficient design.

A design approach based on limit states has the potential to provide cost-effective, safely engineered structures. In order to employ limit states design however, analysis tools must be developed that inform designers of material behavior as it pertains to structural, serviceability and durability issues. Work performed

¹ Graduate Student, Queen's University

² Member ASCE, Professor and Canada Research Chair; GeoEngineering Centre at Queen's-RMC, Kingston Ontario K7L 3N6 moore@civil.queensu.ca; 613 533 3160

³ Professor; Department of Civil Engineering, Queen's University, Kingston, Ontario K7L 3N6 greenm@civil.queensu.ca; 613 533 2128

recently has focused on understanding the non-linear, time-dependent structural behavior of HDPE under different conditions of mechanical loading (Zhang and Moore, 1997). The results have been used to develop non-linear, time-dependent finite element models that accurately predict the behavior of HDPE pipes under various loading conditions (Zhang and Moore, 1997; 1998). However, there remains a dearth of information in the literature regarding the behavior of HDPE pipes under thermal load.

The method of manufacture of HDPE pipe dictates the degree of crystallinity and the orientation of crystals in the material, both of which influence thermal properties (Engeln et. al, 1985; Lacks et al, 1994). In the past, tests have been performed to determine the coefficient of thermal expansion of polyethylene, but investigators have attempted to test only crystalline parts of small samples. Davis et. al (1970) performed tests on coupons specially prepared to achieve a high degree of crystallinity. Jayanna et. al (1993) performed similar tests, but that work investigated the coefficient of thermal expansion of samples of unspecified dimensions along an unspecified axis, and therefore did not address any possible thermal anisotropy. In order to investigate thermal behavior in a manner that is relevant to those developing limit states design methods, testing must be performed on HDPE pipe in an as-received condition.

The primary objective of the present work is to characterize the coefficient of thermal expansion in the longitudinal and circumferential directions for HDPE pipe. The results are to be used in the development of a Finite Element Model that predicts the behavior of HDPE pipes under thermal loading. Such models have the potential to provide greater understanding of failure mechanisms resulting from changing temperature. With greater understanding of these failure mechanisms, limit states design approaches will eventually be possible, allowing HDPE to be used in fully effective pipe design.

Problem Statement

Work is ongoing to implement thermal modeling capability in an existing linear viscoelastic Finite Element Model. In order to properly use Finite Element Analysis to model the behavior of HDPE under thermal loading, five key issues must be investigated. Firstly, it is necessary to determine if the coefficient of thermal expansion (CTE) for HDPE is constant over the temperature range of interest, or whether it in fact varies over that temperature range. Secondly, is the CTE identical in the circumferential and longitudinal directions for any given pipe? Thirdly, does the Standard Dimension Ratio ($SDR = \text{outer diameter divided by wall thickness}$) of a pipe have any effect on the CTE of a given grade and class of HDPE? Fourthly, will a cylindrical pipe give an axisymmetric response under uniform thermal conditions? Fifthly, does the thermal loading history of a pipe affect its response to changing temperature? The following sections address the experimental investigation of these five issues.

All testing to be reported in this paper has been performed on unrestrained HDPE pipe specimens. The results provide part of the parameter data necessary for building a Finite Element Model; however it does not provide the necessary

information to check the predictions made by such a model. To obtain such information, future testing will be performed on restrained specimens.

Test Methodology

Experimental work was performed on two HDPE extruded pipe specimens. One specimen was an 1100mm (43.3 in.) long, 323mm (12.7 in.) outer diameter plain pipe with an SDR of 26. The other specimen was an 1100mm (43.3 in.) long, 206mm (8.1 in.) outer diameter plain pipe with an SDR of 9. The specimens shall herein be referred to as SDR26 and SDR9, respectively. Both specimens were extruded from HDPE with a specific gravity of approximately 0.95 and classified as PE 345434C according to ASTM D3350-93. Both specimens were suspended in a temperature controlled room to allow unrestrained expansion and contraction in the longitudinal and circumferential directions due to temperature change.

Thermally induced strains were applied to both specimens by decreasing the air temperature of the room. Thermal loading consisted of three periods of temperature decrease. During phase I, the temperature was decreased by approximately 30°C in three increments. Phase II and phase III each consisted of a single increment, during which the temperature was decreased by approximately 20°C; the results of phases II and III were used to identify any dependence of thermal strain on thermal loading history. Throughout the test, temperature was measured at several points along the surface of both specimens. The average temperatures on the surface of each specimen at the beginning and end of each increment are summarized in Table 1 below.

Table 1. Summary of Initial and Final Average Air Temperatures

		Temperature (°C)			
		SDR26		SDR9	
		Increment	Initial	Final	Initial
Phase I	1	20	12	20	12
	2	12	1	12	0
	3	1	-10	0	-11
Phase II	4	11	-10	11	-11
Phase III	5	13	-9	12	-9

Linear potentiometers (LPs) were used to measure longitudinal and diametric contraction. For the SDR26 specimen, one LP was used to make longitudinal measurements, and two LPs, oriented at right angles, were used to make diametric measurements. The two diametrically oriented LPs were placed within 50mm of each other, with respect to the longitudinal direction of the specimen, so that any non-axisymmetric response could be identified. For the SDR9 specimen, one LP was used to make longitudinal measurements, and one LP was used to make diametric measurements.

Longitudinal strain is a function of length change such that $\epsilon_{\text{long}} = \Delta_{\text{length}} / \text{length}$. Circumferential strain is a function of diametric change such that

$\epsilon_{\text{circ}} = \Delta_{\text{diameter}} / \text{diameter}$. Thus, longitudinal and circumferential strains were derived from the measurements acquired from the longitudinally and diametrically oriented LPs, respectively.

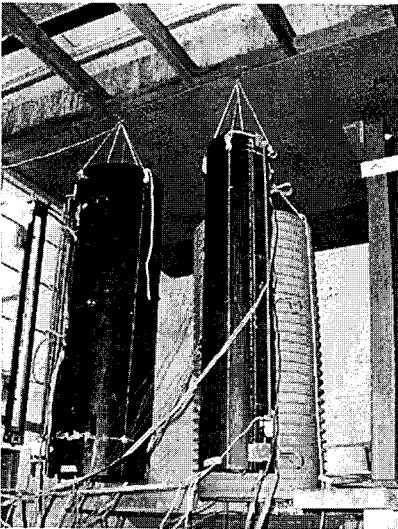
Five rosettes were affixed to each specimen to perform local strain measurements. Strain gauge positioning was as follows. Near each end, one strain gauge was applied to the exterior surface, and one strain gauge was applied to the interior surface; at midpoint, one strain gauge was applied to the exterior surface of the specimen.

Throughout the experiment, air temperature was measured at the surface of each specimen. Temperature measurements were made with integrated circuit temperature transducers (ICs). Five ICs were applied to different locations along the length of each specimen in order to identify the presence of temperature gradients. Each IC was applied within 25mm of a corresponding strain gauge so that any effects due to the presence of temperature gradients could be accounted for in strain gauge results. The test setup and instrument configuration are illustrated in Figure 1 below.

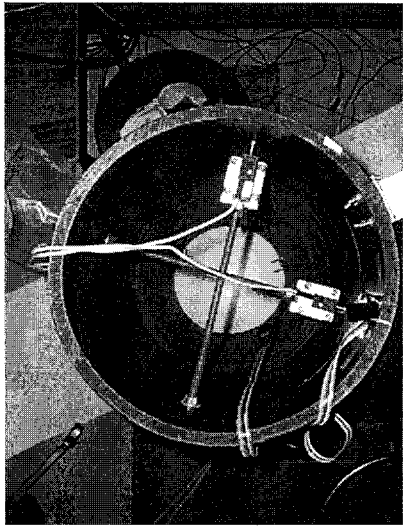
Results and Discussion

Characterization of Coefficients of Thermal Expansion

For each loading increment, the air temperature in the testing room was decreased. Contraction in the longitudinal and circumferential directions was recorded by the



Specimens suspended in cold room



Diametrically oriented LPs in SDR26

Figure 1. Test Setup and Instrument Configuration

LPs and the strain gauges at one second intervals during the course of each of the five thermal loading increments. Strains were then derived from the LP measurements and compared to the strain gauge measurements. The strains recorded by the strain gauges were significantly smaller than those calculated from the LP measurements. This result is attributable to the local stiffening effects created by the glue with which the strain gauges were fixed to the pipes. In order to accurately use strain gauges to measure thermal strains in polyethylene, some stiffening factor must be calculated and applied to the collected strain gauge data. That calculation has not been performed in the present work, and therefore all strains mentioned herein will refer to LP derived strains unless stated otherwise. LP derived strains and measured strains are shown in Figure 2a to illustrate the effect of local stiffening on the strain gauges. For clarity, only the strains derived from the longitudinal LP (for SDR26) and measurements taken from the strain gauge fixed to the middle of the SDR26 specimen are shown. In Figure 2b, temperatures recorded on the surface of the SDR26 specimen are plotted against time; comparison between Figure 2a and Figure 2b shows that the pipe responded quickly to temperature change. For Figure 2a and Figure 2b, only increment 1 is used; subsequent increments showed similar pipe response.

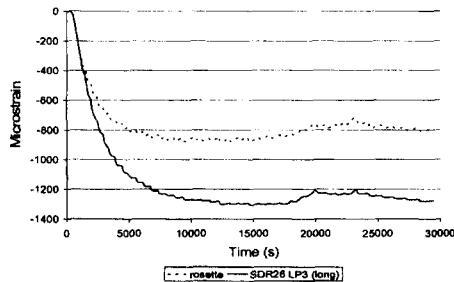


Figure 2a. Comparison of Strains Measured by Strain Gauges and Strains Derived From LP Readings (Increment 1)

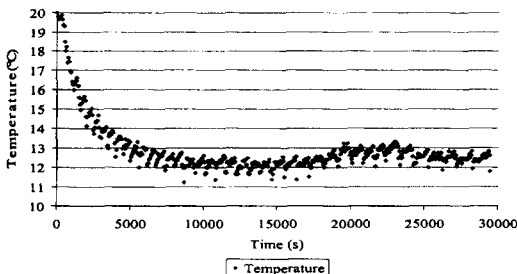
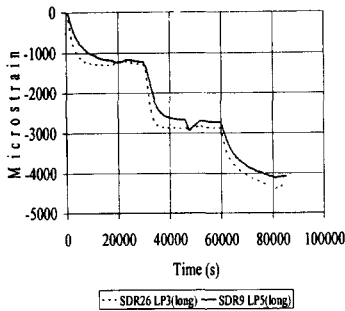
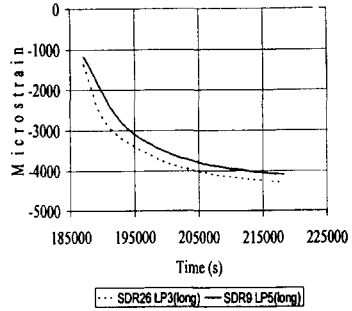


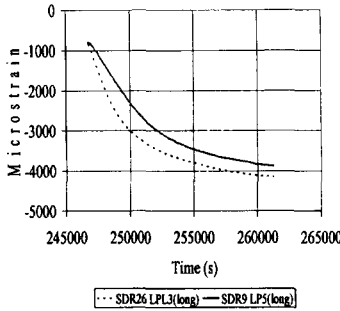
Figure 2b. Temperatures Recorded on the Surface of SDR26 Specimen (Increment 1)



3a. Results for Phase I



3b. Results for Phase II



3c. Results for Phase III

Figure 3a, b, c. LP Derived Strains versus Time – Phases I, II, III

The LP derived thermal strains are plotted against time in Figure 3 to illustrate the length of the cooling periods. For clarity, only longitudinal strains are shown for each sample in Figure 3. The times shown in Figure 3 are measured with $t = 0$ at the beginning of phase I, for all phases.

The LP derived strains from the end of the first three loading increments were plotted against recorded average air temperatures taken at the end of those increments. The results are summarized in Figure 4.

A straight line was fitted to the calculated strains using the method of least squares. This method yielded R-squared values in the range of 0.9945 to 0.9988. Because the strain-temperature curve very closely approximates a linear relationship, it is reasonable to assume that the CTE for the two specimens used in this test is constant over the temperature range -10 to $+20^{\circ}\text{C}$. The CTE is then taken to be the slope of the trend-lines fitted to the data in Figure 4. The CTE values in the longitudinal and circumferential directions are summarized for each specimen, together with corresponding R-squared values, in Table 2. In Table 2,

Circumferential 1 and Circumferential 2 refer to the circumferential CTE calculated for the SDR26 specimen, based on data obtained from the two different LPs used to measure diametric contraction during thermal loading.

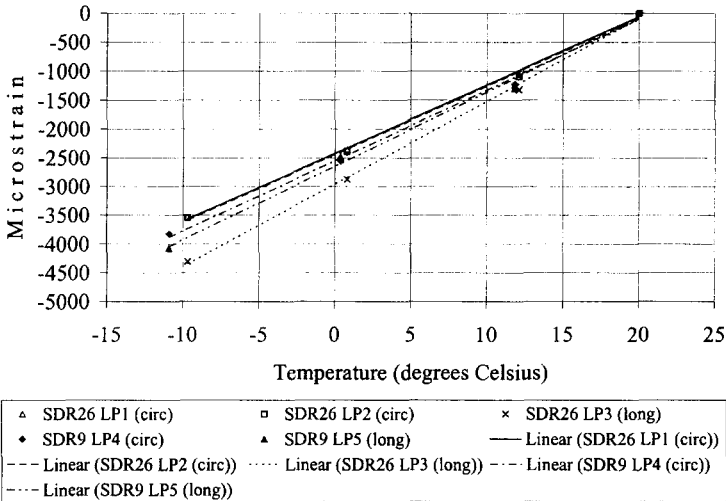


Figure 4. Experimental Results – Final Strains versus Temperature (Phase I)

Table 2. Summary of Coefficients of Expansion

		CTE (mm/mm/°C)	R- squared
SDR26	Longitudinal	1.44×10^{-4}	0.9980
	Circumferential 1	1.18×10^{-4}	0.9988
	Circumferential 2	1.18×10^{-4}	0.9977
SDR9	Longitudinal	1.28×10^{-4}	0.9945
	Circumferential	1.23×10^{-4}	0.9962

Previous researchers have shown that thermally induced strains in polyethylene are not linear with respect to temperature over the range -270 °C to +55 °C. (Davis, 1970) However, based on the R-squared values presented in Table 2, the error associated with assuming a linear relationship is very small for the temperature regime -10 °C to +20 °C. Thus it is readily apparent that, for practical purposes, the CTE may be assumed to be constant when within this temperature range. However, when temperatures exceed these limits, it may not be reasonable to assume a constant CTE.

Thermal Isotropy

Inspection of Figure 4 and Table 2 reveals that some anisotropy exists in the SDR26 specimen, for which the longitudinal CTE is 18% greater than the circumferential CTE. For the SDR9 specimen, the longitudinal CTE is only 4% greater than the circumferential CTE. The difference between the anisotropic responses of the two specimens may be a result of anisotropy of HDPE pipes being some function of SDR, with a higher SDR corresponding to higher anisotropy.

For the SDR9 specimen, the differences in the CTE values are within the bounds of expected experimental error. Therefore, more testing is required before it can be stated confidently that anisotropy indeed exists in that specimen.

Comparison of SDR26 and SDR9

A comparison of strains experienced by the two pipe specimens during the experiment reveals that both possessed circumferential CTEs nearly equal in magnitude. The circumferential CTE for the SDR9 specimen was only 4% greater in magnitude than the corresponding value for the SDR26 specimen. In contrast, the longitudinal CTE for the SDR26 specimen was 11% greater than the corresponding value for the SDR9 specimen. Two implications relevant to future thermal modeling of HDPE pipes are made apparent by these observations. Firstly, it appears reasonable to assume that the CTE in the circumferential direction for HDPE pipes may be taken to be independent of SDR. Secondly, the CTE in the longitudinal direction for HDPE pipes may need to be modeled as some function of SDR. The nature of the relationship between the longitudinal CTE and SDR for a given pipe specimen is a possible avenue of future research.

Thermal Axisymmetry

Diametric measurements made by the two LPs oriented at 90° to each other on the SDR26 specimen agreed perfectly. This result indicates that thermal expansion and contraction of completely unrestrained HDPE pipes may be appropriately assumed to be an axisymmetric phenomenon. Of more practical relevance, this suggests that for any axisymmetric restraint conditions, future thermal modeling may be significantly simplified by the use of axisymmetric analysis as opposed to fully three-dimensional analysis.

Dependence of Thermal Strain on Thermal History

Results recovered from data obtained in phases II and III indicate that thermal strain may be unaffected by thermal loading history. Strains calculated from measurements obtained from increments 3, 4 and 5 were very close in magnitude. These results are summarized in Table 3. In Table 3, the headings LP1, LP2, etc., refer to the instruments that made the measurements from which the corresponding strain values were derived.

Table 3. Final Measured Microstrains for SDR26 and SDR9 Subjected to Further Thermal Loading

Final Microstrains							
SDR26					SDR9		
Increment	Temp (°C) ¹	LP1 (circ)	LP2 (circ)	LP3 (long)	Temp (°C) ²	LP4 (circ)	LP5 (long)
0	20	0	0	0	20	0	0
3	-10	-3539	-3547	-4307	-11	-3829	-4078
4	-10	-3525	-3534	-4295	-11	-3816	-4093
5	-9	-3413	-3476	-4151	-9	-3603	-3881

1 Averages of temperatures measured on surface of SDR26

2 Averages of temperatures measured on surface of SDR9

Because of limitations on the precision of temperature control in the testing room, it was not possible to obtain three exactly identical temperatures in each of the three phases for the purposes of comparison. Therefore, the following method is used for comparison between the values summarized in Table 3. Using the trend of results from the phase I testing, presented in Figure 4, strain values were calculated at each of the temperatures obtained in phases II and III. The predicted values were then compared to the measured values, and the percentage strain difference was then calculated. The results are summarized in Table 4.

Table 4. Comparison of Measured and Calculated Microstrains for Phase II and III

	Instrument	Phase	Calculated Microstrain	Measured Microstrain	% Difference
SDR26	LP1 (circ)	II	-3548	-3525	0.6
		III	-3430	-3413	0.5
	LP2 (circ)	II	-3570	-3534	1.0
		III	-3452	-3476	0.7
	LP3 (long)	II	-4326	-4295	0.7
		III	-4182	-4151	0.8
SDR9	LP4 (circ)	II	-3927	-3816	2.9
		III	-3707	-3603	2.9
	LP5 (long)	II	-4087	-4093	0.2
		III	-3855	-3881	0.7

Using this method, the largest strain difference, that for the circumferential strain of the SDR9 specimen, was 2.9%; the smallest strain difference, that for the longitudinal strain of the SDR9 specimen, was 0.2%. The results of this comparison indicate that, for an HDPE pipe that has been subjected to the range of temperatures used during this test, it is reasonable to assume that thermal loading history has no effect on contraction due to temperature decrease.

Conclusions

The longitudinal and circumferential CTE for the SDR26 specimen were found to be $1.44 \times 10^{-4} \text{ } ^\circ\text{C}^{-1}$ and $1.18 \times 10^{-4} \text{ } ^\circ\text{C}^{-1}$ respectively. The longitudinal and

circumferential CTE for the SDR9 specimen were found to be $1.28 \times 10^{-4} \text{ }^\circ\text{C}^{-1}$ and $1.23 \times 10^{-4} \text{ }^\circ\text{C}^{-1}$ respectively. It was found that the CTE for both specimens may be appropriately assumed to be constant over the temperature range -10°C to $+20^\circ\text{C}$. The SDR26 specimen was found to be thermally anisotropic. Thermally anisotropic response was detected in the SDR9 specimen as well; however it was minor enough to warrant further testing to determine its significance. A comparison between the two specimens revealed that both showed nearly equal circumferential CTE, but measurements showed the SDR26 specimen to have a significantly greater longitudinal CTE than the SDR9 specimen. Results from tests featuring repeated thermal loading indicated that it is reasonable to assume that thermal loading history has no effect on the material contraction after any specific temperature decrease.

Acknowledgements

This work has been supported by Natural Sciences and Engineering Research Council of Canada through research funds granted to Dr. Ian Moore. Dr. Moore's position at Queen's University is funded by the Canadian Government through the Canada Research Chairs Program.

References

Zhang, C., and I.D. Moore. Nonlinear Mechanical Response of High Density Polyethylene, Part I: Experimental Investigation and Model Evaluation. *Polymer Engineering and Science*, Vol. 37. 1997, pp. 404-413.

Zhang, C.; Moore, I.D. Nonlinear Mechanical Response of High Density Polyethylene, Part II: Uniaxial Constitutive Modeling. *Polymer Engineering and Science*, Vol. 37. 1997, pp. 414-420.

Zhang, C.; Moore, I.D. Nonlinear Finite Element Analysis for Thermoplastic Pipes. *Transportation Research Record - 1624*. September 1998, pp 225-230.

Engeln, I.; Meissner, M.; Pape, H.E. Thermal Expansion and Gruneisen Parameter of Polyethylene between 5 and 320K *Polymer*, Vol. 26, 1985, p. 364

Lacks, D.J.; Rutledge, G.C. Simulation of the Temperature Dependence of Mechanical Properties of Polyethylene *Journal of Physical Chemistry*, Vol. 98, 1994, p. 1222

Davis, G.T; Eby, R.K.; Colson, J.P. Thermal Expansion of Polyethylene Unit Cell: Effect of Lamella Thickness *Journal of Applied Physics*, Vol. 41, 1970, p. 4316

Jayanna, H.S.; Subramanyam, S.V Thermal Expansion of Irradiated Polyethylene from 10 to 340K *Journal of Physical Chemistry*, Vol. 31, 1993, p. 1095